Oceanologia (2020) 62, 56—69

Available online at www.sciencedirect.com

ScienceDirect

journal homepage: www.journals.elsevier.com/oceanologia/

ORIGINAL RESEARCH ARTICLE

Evaluation of the carbon sequestration capacity of arid mangroves along nutrient availability and salinity gradients along the Red Sea coastline of Saudi Arabia

Kamal H. Shaltout [a], Mohamed T. Ahmed [a,b], Sulaiman A. Alrumman [b], Dalia A. Ahmed [a], Ebrahem M. Eid [b,1,*]

[a] *Botany Department, Faculty of Science, Tanta University, Tanta, Egypt*
[b] *Biology Department, College of Science, King Khalid University, Abha, Saudi Arabia*

Received 24 April 2019; accepted 22 August 2019
Available online 12 September 2019

KEYWORDS
Carbon sequestration;
Coastal wetlands;
Mangroves;
Red Sea;
Saudi Arabia;
Climate change

Summary In the present work, we assessed the carbon sequestration capacity of mangrove forests (*Avicennia marina*) in relation to nutrient availability and salinity gradients along the Red Sea coast of Saudi Arabia. This was achieved through estimating the sediment bulk density (SBD), sediment organic carbon (SOC) concentration, SOC density, SOC pool, carbon sequestration rate (CSR) and carbon sequestration potential (CSP). The present study was conducted at 3 locations (northern, middle and southern), using 7 sites and 21 stands of mangrove forests (*A. marina*) along ~1134 km of the Red Sea coastline of Saudi Arabia (from Duba in the north to Jazan in the south), all of which are in an arid climate. The correlation coefficients between the water characteristics and the first two Canonical Correspondence Analysis (CCA) axes indicated that the separation of the sediment parameters along the first axis were positively influenced by TDS (total dissolved solids) and EC (electric conductivity) and were negatively influenced by total N and total P. On the other hand, the second axis was negatively correlated with total N, total P, EC and TDS. The SOC pools at the northern (10.5 kg C m^{-2}) and southern locations (10.4 kg C m^{-2}) were significantly

* Corresponding author at: Botany Department, Faculty of Science, Kafr El-Sheikh University, Kafr El-Sheikh 33516, Egypt. Tel.: +966 55 2717026; fax: +966 17 241 8205.
E-mail addresses: ebrahem.eid@sci.kfs.edu.eg, eeid@kku.edu.sa, ebrahem.eid@gmail.com (E.M. Eid).
[1] Permanent address: Botany Department, Faculty of Science, Kafr El-Sheikh University, Kafr El-Sheikh, Egypt.
Peer review under the responsibility of Institute of Oceanology of the Polish Academy of Sciences.

ELSEVIER | Production and hosting by Elsevier

https://doi.org/10.1016/j.oceano.2019.08.002

higher than the SOC pool at the middle location (6.7 kg C m^{-2}). In addition, the average CSR of the northern (5.9 g C m^{-2} yr^{-1}) and southern locations (6.0 g C m^{-2} yr^{-1}) were significantly higher than they were in the middle location (5.0 g C m^{-2} yr^{-1}).

1. Introduction

Carbon dioxide (CO_2) is one of the greenhouse gases, and it plays a major role in climate change and global warming, where its concentration increased from 280 ppmv in 1850 to 411 ppmv in 2019 (Page, 2019); thus, many scientists have suggested that CO_2 sequestration in soil organic carbon may significantly contribute to reducing the effects of climate change (Alongi, 2012, 2014; Siikamäki et al., 2012; Taillardat et al., 2018). Furthermore, increasing soil carbon pools and protecting carbon rich soils are key for achieving the Paris Climate Agreement's climate targets (Rumpel et al., 2018).

Mangroves are one of the most important blue carbon ecosystems because they act as a carbon sink and contribute to the mitigation of atmospheric greenhouse gas emissions (Taillardat et al., 2018). Mangroves cover approximately 137,600 km^2 in 118 countries (Bunting et al., 2018); they are typically composed of shrubs and trees and form extensive forested wetlands along both muddy and carbonate coasts in tropical and subtropical climates (Rovai et al., 2018; Twilley et al., 2018). They usually grow in estuaries where nutrients are plentiful; they also grow in nutrient-poor areas such as carbonate coasts in the Caribbean and Red Sea regions where trees are dwarfed (Lovelock et al., 2004). Compared to terrestrial carbon pools, mangroves store more sedimentary carbon per area than any other terrestrial ecosystem (Twilley et al., 2018), where mangrove sediments contain up to 36.1 kg m^{-2} of blue carbon within the top 1 m of sediment (Sanderman et al., 2018). This amount is much greater than soil carbon pools estimated for other ecosystems such as closed shrublands (11.0 kg m^{-2}), savannas (11.2 kg m^{-2}), croplands (12.7 kg m^{-2}), deciduous broadleaf forests (13.4 kg m^{-2}), evergreen broadleaf forests (15.1 kg m^{-2}), grasslands (15.5 kg m^{-2}), open shrublands (16.9 kg m^{-2}), mixed forests (19.8 kg m^{-2}), evergreen needleleaf forests (21.0 kg m^{-2}), permanent wetlands (24.1 kg m^{-2}), and deciduous needleleaf forests (25.3 kg m^{-2}) (Sanderman et al., 2018). Mangroves also provide many beneficial environmental services to coastal communities (Almahasheer et al., 2017) such as protection of the coast from winds, erosion, and provision of food and shelter for many types of marine life and birds (Eid et al., 2016; Shaltout, 2016).

Mangrove forests are one of the most threatened ecosystems due to urban expansion and other land uses; thus, understanding the distribution of soil carbon in mangrove forests is very important for prioritizing protection and restoration efforts for climate mitigation (Sanderman et al., 2018). In the Arabian Peninsula, mangrove forests are found along its east and west coasts (Kumar et al., 2010). The Red Sea is near the northern limit of mangroves in the Indo-Pacific region, situated in the Sinai Peninsula at 28°N (Almahasheer et al., 2016a). The harsh environment of the Red Sea region is considered a limiting agent for the growth and prosperity of mangroves (Edwards and Head, 1987). However, the area of Red Sea mangroves (135 km^2) has increased by 12% over the past forty years, which may be attributed to repairing and afforestation projects (Almahasheer et al., 2016a). Mangrove forests of the Red Sea include examples of euhaline-metahaline and hard-bottomed mangroves (Price et al., 1987). Kumar et al. (2010) reported that the mangroves along the Saudi Arabian Red Sea coast are found as fragmented stands in intertidal zones. Price et al. (1998) reported that mangroves of the Saudi Arabian Red Sea coast were significantly more abundant along coastal sites than offshore sites, as well as more abundant in southern latitudes compared to northern latitudes. This type of vegetation is of special interest as it flourishes in the most unfavourable conditions, such as areas with high salinity, devoid of rivers, scarce rainfall and dry land (Saifullah, 1994). *Avicennia marina* in Saudi Arabia, covers approximately 48.4 km^2 along the Red Sea coast (Almahasheer, personal communication), and some 10.4 km^2 along the Arabian Gulf (Almahasheer, 2018). On the Red Sea coast of Saudi Arabia, mangrove stands extend from the Jordanian border in the north to the southern border in Jazan (El-Juhany, 2009) but are not continuous due to severe environmental conditions (Saifullah, 1997).

Some studies have been conducted to assess the carbon sequestration potential (CSP) of mangrove forests along the Saudi Arabian Red Sea coast and all these studies were carried out in southern locations and only one was carried out in a central location. Eid et al. (2016) explored the efficiency of mangrove forests along the southern Saudi Arabian Red Sea coast for CSP. Almahasheer et al. (2017) assessed the sediment organic carbon (SOC) pools and carbon sequestration rate (CSR) in mangroves along the central Saudi Red Sea coast. Arshad et al. (2018) evaluated the CSR in polluted and non-polluted mangrove sediments near Jazan, an urban city (southern Saudi Red Sea coast). Eid et al. (2019) evaluated the impact of land use changes due to conversion of areas of mangrove growth to shrimp farms on the SOC pool in the sediment along the southern Saudi Red Sea coast.

As a result of human activities, nutrient availability varies from north to south along the Saudi Red Sea coast today. Moreover, salinity in Red Sea surface water increases northwards (Edwards, 1987). To our knowledge, no study has been carried out in Saudi Arabia to evaluate the carbon sequestration capacity of mangrove forests along nutrient availability and salinity gradients along the entire Saudi Red Sea coast. Thus, the present study was carried out to evaluate sediment bulk density (SBD), SOC concentration, SOC density, the SOC pool, the CSR and CSP in the mangrove sediments along nutrient availability and salinity gradients along

~1134 km of the Saudi Arabian Red Sea coastline (from Duba in the north to Jazan in the south). Hence, the goal of the current investigation was to evaluate probable changes in "blue carbon" due to nutrient availability and salinity effects. The results of this study have worldwide applications because they can be extrapolated to similarly high-value ecosystems to mitigate carbon emissions in other parts of the planet and serve to mitigate their degradation.

2. Material and methods

2.1. Study area

The Red Sea coast of Saudi Arabia extends in the NW-SE direction to a distance of 1700 km and lies between the northern end of the Gulf of Suez at a latitude of 30°N and the southern end at Bab El-Mandeb at approximately 13°N (Fig. 1) (Saifullah, 1997). The climate of Saudi Arabia is arid and very severe with high temperatures and minimal rainfall (Siraj, 1984). Winds are northerly in winter and southerly in summer (Morley, 1975). Rainfall in southwestern Saudi Arabia is caused by monsoons formed in the Indian Ocean; thus, rainfall increases significantly from north to south (Eid et al., 2016). Red Sea surface temperatures increase southward, while surface water salinity increases northwards (Edwards, 1987). *Avicennia marina* (Forssk.) Vierh. is the dominant species in mangrove forests along the Saudi Red Sea coast, while *Rhizophora mucronata* Lam. can be found only in scattered patches in the Farasan Islands (Mandura et al., 1987). According to El-Juhany (2009), mangrove forests have been subjected to many stresses, such as camel grazing, trash in the sea and on the beaches, and the establishment of other human activities such as shrimp farms.

2.2. Sampling locations

Sampling was carried out (supplementary material 1) at 3 locations (northern, middle and southern), 7 sites and in 21 stands of mangrove forests (*A. marina*) along the Saudi Arabian Red Sea coast (Fig. 1). The distance between the northern and middle location is 736 km and the distance between the middle and southern location is 398 km. The northern location is characterized by high salinity, relatively low temperatures, dry land and minimal rainfall (Saifullah, 1997). The middle location is characterized by extreme climatic conditions such as high temperatures and sporadic rainfall (Almahasheer et al., 2016b); furthermore, eutrophication is occurring as the result of sewage and fertilizer discharging into the sea which affects mangrove growth (Almahasheer et al., 2017). The southern location is characterized by low salinity, favourable temperatures, soft muddy soil, plentiful rainfall and an abundance of nutrients (Saifullah, 1997). Sampling in the northern and middle locations occurred at one site with three mangrove stands (Duba and Jeddah Cities, respectively), while in the southern location sampling occurred at 5 sites with 15 mangrove stands (three per site) (Fig. 1).

2.3. Sediment sampling

Sampled stands were selected to cover mangroves' habitats evenly to enable an accurate evaluation of mangroves' capacity to sequester carbon along the Saudi Red Sea coast. A total of 187 sediment cores were collected from 21 sampled stands to ensure a proper estimate of carbon sequestration in mangrove sediments. The sediment samples were collected with a 7 cm diameter hand sediment corer, which provides a

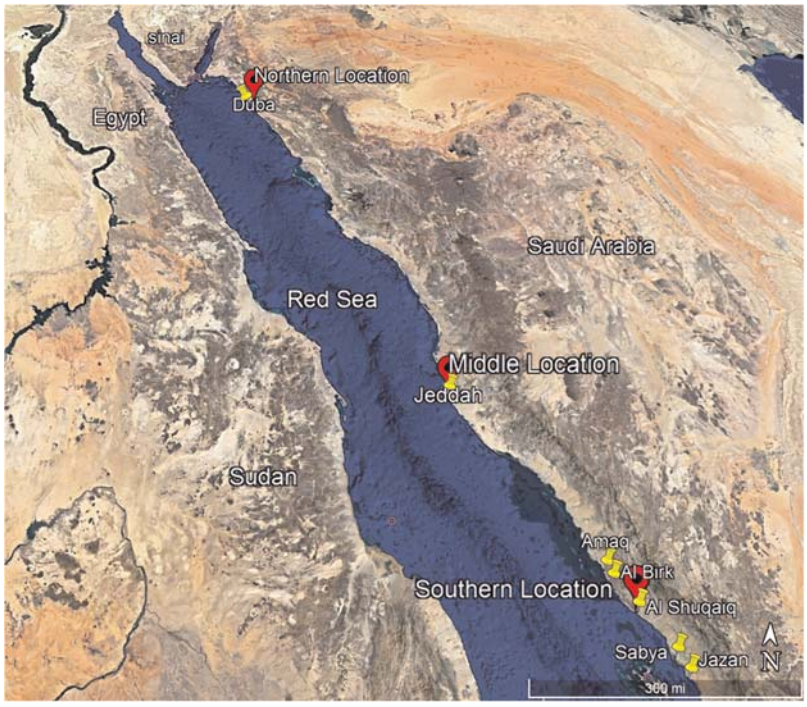

Figure 1 Map of the study area indicating the 3 locations [📍] and the 7 sampling sites [📌].

perfect sediment core (Tan, 2005). The corer was pushed down to a depth of 50 cm, and then the sediment core was removed from the corer carefully. The sediment core was immediately sectioned with a blade into 10 samples each of 5 cm thick (0–5, 5–10, 10–15, 15–20, 20–25, 25–30, 30–35, 35–40, 40–45 and 45–50 cm) and packed in plastic containers. The sample containers were tightly sealed and stored on ice to avoid volatilization losses and to minimize microbial activity until analysis (Eid and Shaltout, 2016). Thus, 1383 sediment samples were collected to determine SBD, SOC concentration, SOC density and the SOC pool.

2.4. Population characteristics

At each sampling stand, population density, height, and crown diameter of all mangrove trees (*A. marina*) were estimated inside three randomly distributed quadrates (each of 10 × 10 m).

2.5. Sediment analysis

Each sediment sample was oven-dried at 105°C for three days, cooled in a desiccator, and weighed to determine SBD as follows (Wilke, 2005):

$$\rho_{sj} = \frac{m_j}{v_j},$$

where ρ_{sj} is SBD [g cm^{-3}] of the j^{th} layer, m_j is mass of sediment sample [g] of the j^{th} layer dried at 105°C, and v_j is the volume of the sediment sample [cm^3] of the j^{th} layer. Dry samples were grinded and sieved to pass through a 2 mm mesh size. Nóbrega et al. (2015) recommended using the loss on ignition method to estimate SOC in mangrove sediments in the absence of a CHN analyser. Thus, each sample was analyzed for SOC concentration by measuring sediment organic matter (SOM) using the loss on ignition method at 550°C for two hours as follows (Jones, 2001): SOM concentration [g C kg^{-1}] = 1000 × (weight of oven dried sample [g] − weight of sample after ignition [g])/weight of oven dried sample [g]); SOC [g C kg^{-1}] = 0.5 × SOM [g C kg^{-1}] (Pribyl, 2010).

SOC density [kg C m^{-3}] was estimated as follows (Han et al., 2010): $SOC_{dj} = \rho_{sj} \times SOC_j$, where SOC_{dj} is the SOC density [kg C m^{-3}] of the j^{th} layer, ρ_{sj} is the SBD [g cm^{-3}] of the j^{th} layer, and SOC_j is the SOC concentration [g C kg^{-1}] of the j^{th} layer.

SOC pool [kg C m^{-2}] of a profile, expressed as a mass per unit surface area to a fixed depth, was calculated as follows (Meersmans et al., 2008):

$$SOC_p = \frac{\sum_{j=1}^{k} SOC_{dj} \times T_j}{\sum_{j=1}^{k} T_j} \times D_r,$$

where SOC_p is the SOC pool [kg C m^{-2}], D_r is the reference depth (=0.5 m), T_j is the thickness [m] of the j^{th} layer and k is the number of the layers. CSR [g C m^{-2} yr^{-1}] was estimated based on the sedimentation rate, SBD and SOC concentration (Xiaonan et al., 2008):

$$CSR_i = \rho_{si} \times SOC_i \times R,$$

where CSR_i is the CSR [g C m^{-2} yr^{-1}] of the i^{th} location, ρ_{si} is the mean SBD [g cm^{-3}] of the i^{th} location, SOC_i is the mean SOC concentration [%] of the i^{th} location and R is the sedimentation rate in the mangrove forests (the Saudi mean = 2.2 mm yr^{-1}; Almahasheer et al., 2017).

CSP [Gg C year^{-1}] was calculated as follows (Xiaonan et al., 2008):

$$CSP = CSR \times A,$$

where CSP is the CSP [Gg C yr^{-1}] of the mangrove stands and A is the area [m^2] of the mangrove stands.

2.6. Water sampling and analysis

At each stand, three polyethylene bottles (1000 ml) were used to collect water samples during low tide (<0.3 m water depth) from the water surface and were brought to the laboratory. EC (electric conductivity) and TDS (total dissolved solids) were measured immediately after collection using a conductivity meter (Hanna Instruments, HI 98130). Then, samples were filtered using nylon Whatman membrane filters (pore size 0.45 μm, diameter 47 mm). The filtrates were acidified to a pH of 2.0 using nitric acid (Analar) in order to preserve the nutrients in the samples. Molybdenum blue (Strickland and Parsons, 1972) and indo-phenol blue (Novozamsky et al., 1974) methods were applied for the determination of total P and total N, using a spectrophotometer (Perkin Elmer, Lambda 25) at 885 and 660 nm, respectively.

2.7. Statistical analysis

Before performing an analysis of variance (ANOVA), the data were tested for their normality of distribution and homogeneity of variance, and when necessary, the data were log-transformed. One-way analysis of variance (ANOVA-1) was used to identify statistically significant differences in the estimated chemical parameters of seawater, SOC pool, CSR, tree density, individual height and crown diameter of *A. marina* populations among the different studied locations. Two-way analysis of variance (ANOVA-2) was used to identify statistically significant differences in SBD, SOC concentrations and SOC density among the different studied locations and sediment depths. Significant differences between means among the studied locations were identified using Tukey's HSD test at $P < 0.05$. The relationship between SOC concentration and SBD was examined with non-linear regression and by calculating the Pearson correlation coefficient (Arshad et al., 2018; Eid et al., 2019, 2016; Eid and Shaltout, 2016). To detect the ordination of the population (tree density, individual height and crown diameter) and sediment (SBD, SOC concentration, SOC density, SOC pool, CSR and CSP) parameters along the nutrient availability and salinity gradients, Canonical Correspondence Analysis (CCA) was conducted using the population and sediment parameters along with the water properties using CANOCO 5.0 for Windows (Ter Braak and Šmilauer, 2012). Relationships between the ordination axes and the water properties were tested using Pearson's simple linear correlation (r). All statistical analyses were performed using SPSS 15.0 software (SPSS, 2006).

3. Results

For seawater samples, TDS showed a significant concentration gradient, with highest values in the north and lowest

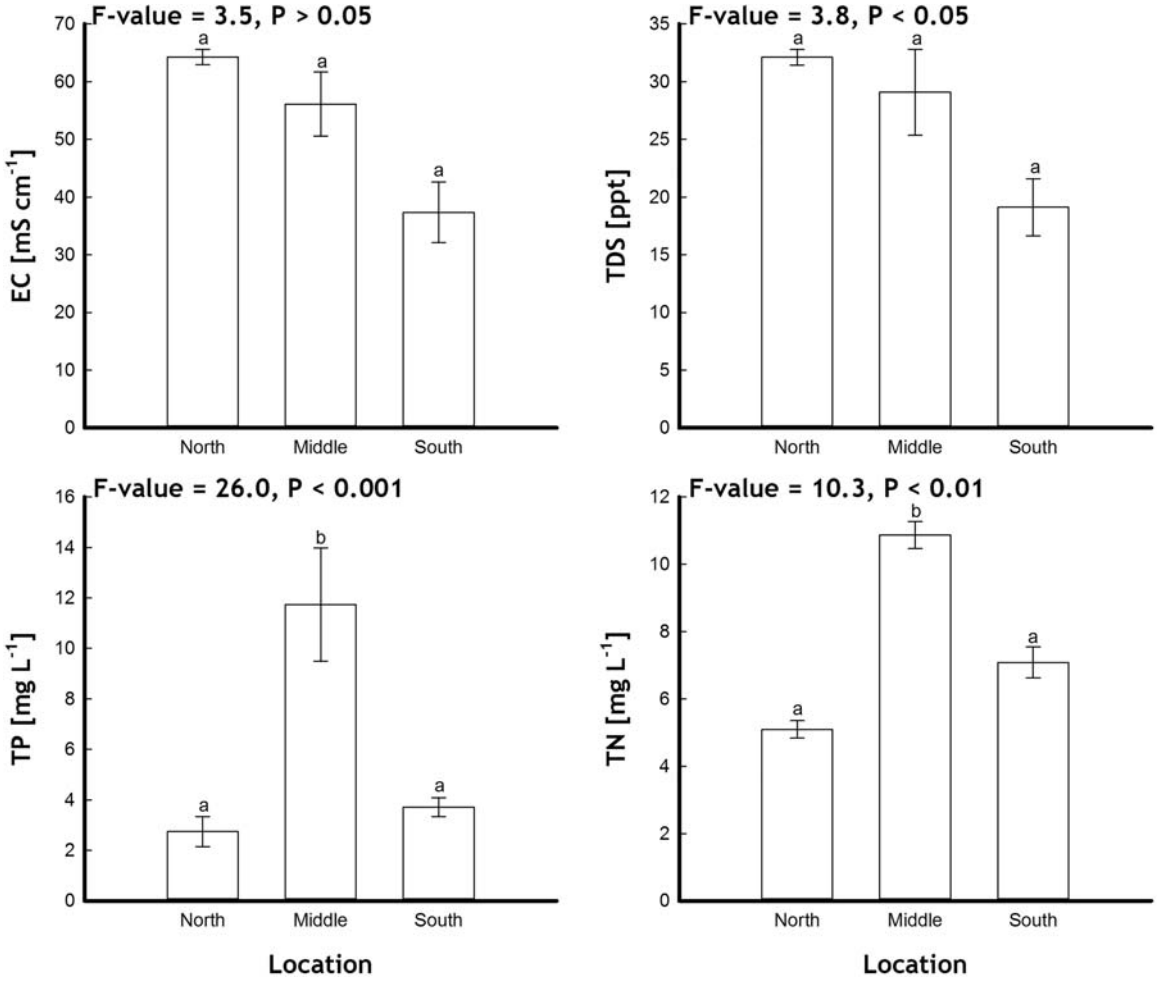

Figure 2 Variation in the water characteristics of the three locations supporting *Avicennia marina* populations along the Red Sea coast of Saudi Arabia. Vertical bars indicate the standard errors of the means. *F*-values represent the one-way ANOVA. Means followed by different letters are significantly different at $P < 0.05$ according to the Tukey's HSD test.

Table 1 Characteristics [mean ± standard error] of *Avicennia marina* populations along the Red Sea coast of Saudi Arabia.

Location	Tree density [ind. 100 m^2]	Tree height [cm ind.$^{-1}$]	Tree crown diameter [cm ind.$^{-1}$]
North	$7.7^{a} \pm 0.9$	$106.1^{b} \pm 6.2$	$100.7^{b} \pm 5.7$
Middle	$26.4^{c} \pm 2.3$	$75.6^{a} \pm 2.4$	$66.5^{a} \pm 3.4$
South	$13.6^{b} \pm 0.7$	$198.6^{c} \pm 4.4$	$226.5^{c} \pm 4.7$
F value	24.4^{***}	173.1^{***}	257.9^{***}

F-values represent the one-way ANOVA, ***: $P < 0.001$. Means in the same columns followed by different letters are significantly different at $P < 0.05$ according to Tukey's HSD test.

values in the south, while EC reflected a similar but insignificant concentration gradient. Total P and total N in seawater samples differed significantly among studied locations, where highest concentrations in the middle, and lowest concentrations in the north (Fig. 2).

The population of *A. marina* in the middle location had the highest tree density (26.4 ind. 100 m^2), but the lowest tree height (75.6 cm ind.$^{-1}$) and crown diameter (66.5 cm ind.$^{-1}$). In contrast, its population in the southern location had the highest tree height (198.6 cm ind.$^{-1}$) and crown diameter (226.5 cm ind.$^{-1}$), but a medium tree density (13.6 ind. 100 m^2) (Table 1). The correlation coefficients between the water characteristics and the first two CCA axes (Fig. 3 and Table 2) indicated that the separation of *A. marina* population parameters along the first axis was positively influenced by total N and total P, while the second axis was negatively correlated with total P.

The correlation coefficients between the water characteristics and the first two CCA axes (Fig. 4 and Table 2) indicated that the separation of the sediment parameters along the first axis were positively influenced by TDS and EC and negatively influenced by total N and total P. In contrast,

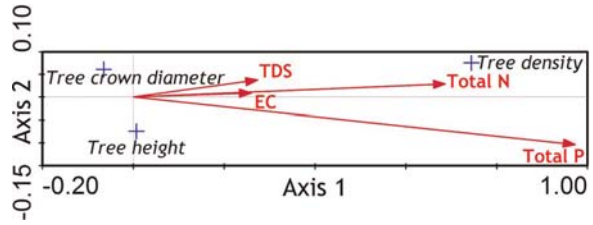

Figure 3 CCA biplot with water characteristics [→] and population parameters [+] of *Avicennia marina* growing along the Red Sea coast of Saudi Arabia.

Table 2 Inter-set correlations of water properties with CCA axes.

Water property	Axis 1	Axis 2
Sediment parameters		
EC [mS cm^{-1}]	0.53	−0.56
TDS [ppt]	0.55	−0.54
Total P [mg L^{-1}]	−0.29	−0.57
Total N [mg L^{-1}]	−0.44	−0.61
Population parameters		
EC [mS cm^{-1}]	0.24	0.01
TDS [ppt]	0.26	0.04
Total P [mg L^{-1}]	0.91	−0.10
Total N [mg L^{-1}]	0.64	0.03

EC: electric conductivity; TDS: total dissolved solids.

the second axis was negatively correlated with total N, total P, EC and TDS. The total mean of SBD, SOC concentration, SOC density, SOC pool and CSR differed significantly among the studied locations (Table 3). The distribution of SBD in the northern location showed higher mean values where it increased significantly from 1.6 g cm^{-3} at a depth of 0–5 cm up to 2.3 g cm^{-3} at a depth of 25–30 cm. On the other hand, the distribution of SBD in the middle location increased significantly from 1.3 g cm^{-3} at a depth of 0–5 cm and up to 1.6 g cm^{-3} at a depth of 10–15 cm. The distribution of mean SBD in the southern location increased significantly from 1.3 g cm^{-3} at a depth of 0–5 cm and up to 1.7 g cm^{-3} at a depth of 30–35 cm (Fig. 5).

SOC concentrations in the southern location showed higher mean values where they declined significantly from 19.7 g C kg^{-1} at a depth of 0–5 cm to 13.7 g C kg^{-1} at a depth of 40–45 cm, while SOC concentrations in the

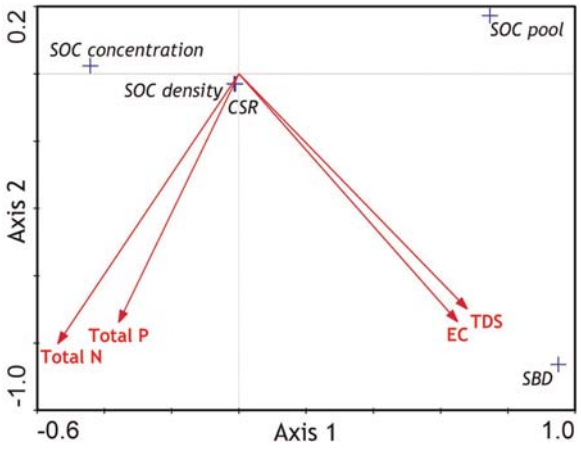

Figure 4 CCA biplot with water characteristics [→] and sediment parameters [+] supporting *Avicennia marina* populations along the Red Sea coast of Saudi Arabia.

middle location declined significantly from 16.7 g C kg^{-1} at a depth of 0–5 cm to 13.6 g C kg^{-1} at a depth of 20–25 cm. In contrast, SOC concentrations in the northern location showed lower mean values, declining significantly from 15.3 g C kg^{-1} at a depth of 0–5 cm to 12.1 g C kg^{-1} at a depth of 20–25 cm (Fig. 6). Consistent with the results, an exponential function was developed between SBD [g cm^{-3}] and SOC concentrations [g C kg^{-1}] for the sediments in Saudi Arabian Red Sea mangroves, where SOC concentrations and SBD were negatively correlated (Fig. 7).

In the northern location, SOC density significantly declined from 27.2 kg C m^{-3} at a depth of 10–15 cm to a minimum of 23.9 kg C m^{-3} at a depth of 20–25 cm then increased to 32.5 kg C m^{-3} at a depth of 30–35 cm, before finally decreasing to 25.4 kg C m^{-3} at a depth of 35–40; SOC density in the southern location significantly decreased from 27.2 kg C m^{-3} at a depth of 5–10 cm to 26.1 kg C m^{-3} at a depth of 10–15 cm, and then it increased to 29.4 kg C m^{-3} at a depth of 30–35 cm and finally decreased to 21.2 kg C m^{-3} at a depth of 45–50 cm. On the other hand, the middle location showed lower mean SOC density values where they significantly decreased from 25.8 kg C m^{-3} at a depth of 10–15 cm to 21.0 kg C m^{-3} at a depth of 20–25 cm (Fig. 8).

The northern and southern locations have similar SOC pools (10.5 and 10.4 kg C m^{-2}, respectively), while the value

Table 3 Mean ± standard error of sediment bulk density [SBD], sediment organic carbon [SOC] concentration, SOC density, SOC pool and carbon sequestration rate [CSR] in the 3 *Avicennia marina* locations along the Red Sea coast of Saudi Arabia.

Location	SBD [g cm^{-3}]	SOC concentration [g C kg^{-1}]	SOC density [kg C m^{-3}]	SOC pool [kg C m^{-2}]	CSR [g C m^{-2} yr^{-1}]
North	1.9^{b} ± 0.04	14.4^{a} ± 0.3	26.9^{b} ± 0.9	10.5^{b} ± 0.5	5.9^{b} ± 0.2
Middle	1.5^{a} ± 0.03	15.9^{b} ± 0.3	22.7^{a} ± 0.5	6.7^{a} ± 0.4	5.0^{a} ± 0.1
South	1.5^{a} ± 0.01	18.1^{c} ± 0.2	27.1^{b} ± 0.3	10.4^{b} ± 0.3	6.0^{b} ± 0.1
F value	42.9***	10.5***	9.1***	17.0***	13.5***

F-values represent the one-way ANOVA, ***: $P < 0.001$. Means in the same columns followed by different letters are significantly different at $P < 0.05$ according to Tukey's HSD test.

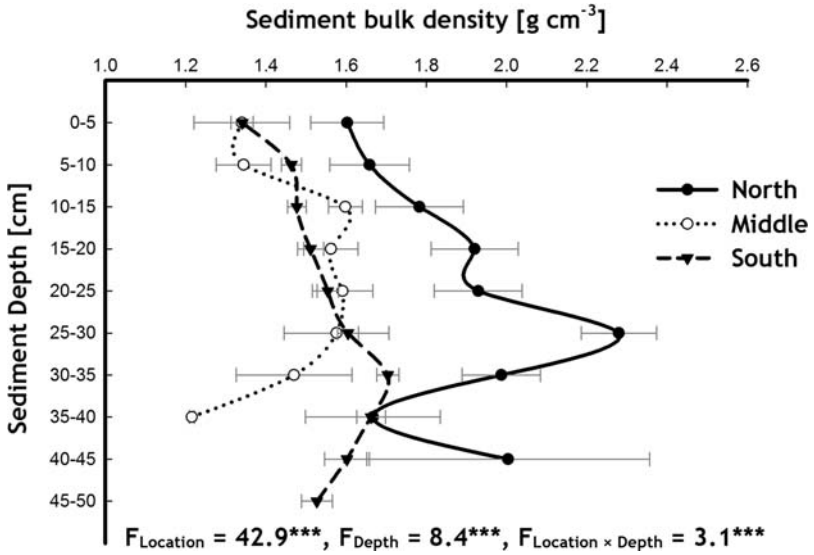

Figure 5 Distribution of sediment bulk density [g cm^{-3}] in relation to sediment depth [cm] in three locations of *Avicennia marina* populations along the Red Sea coast of Saudi Arabia. Horizontal bars indicate the standard errors of the means. *F*-values represent the two-way ANOVAs. Location: North/Middle/South; Depth: 0—5, 5—10, 10—15, 15—20, 20—25, 25—30, 30—35, 35—40, 40—45, 45—50 cm. ***: $P < 0.001$.

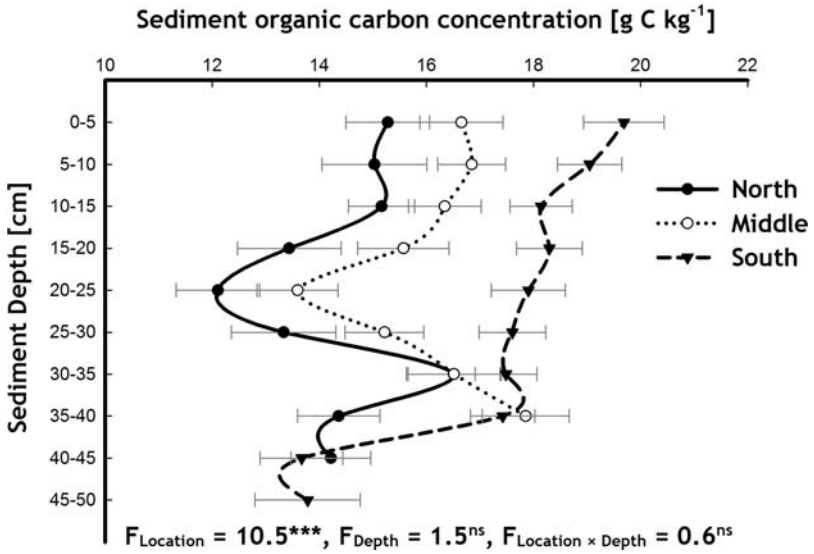

Figure 6 Distribution of sediment organic carbon concentration [g C kg^{-1}] in relation to sediment depth [cm] in three locations of *Avicennia marina* populations along the Red Sea coast of Saudi Arabia. Horizontal bars indicate the standard errors of the means. *F*-values represent the two-way ANOVAs. Location: North/Middle/South; Depth: 0—5, 5—10, 10—15, 15—20, 20—25, 25—30, 30—35, 35—40, 40—45, 45—50 cm. ***: $P < 0.001$, *ns*: not significant [i.e., $P > 0.05$].

of the middle location was 6.7 kg C m^{-2}. In addition, the average CSR of the middle location (5.0 g C m^{-2} yr^{-1}) was significantly lower than those of the northern (5.9 g C m^{-2} yr^{-1}) and southern locations (6.0 g C m^{-2} yr^{-1}) (Table 3). Based on the area of the mangrove stands (48.4 km^2) in the study area and the CSR, the total CSP of mangrove forests along the Saudi Arabian Red Sea coast was 0.27 Gg C yr^{-1}.

4. Discussion

The present results indicate that SOC concentrations were adversely affected by the increase in total P and total N. On the other hand, SBD was positively affected by higher EC and TDS. Salinity and nutrient abundance have been shown to affect the productivity of mangroves. High salinity levels can result in physiological stress to mangrove trees, forcing them

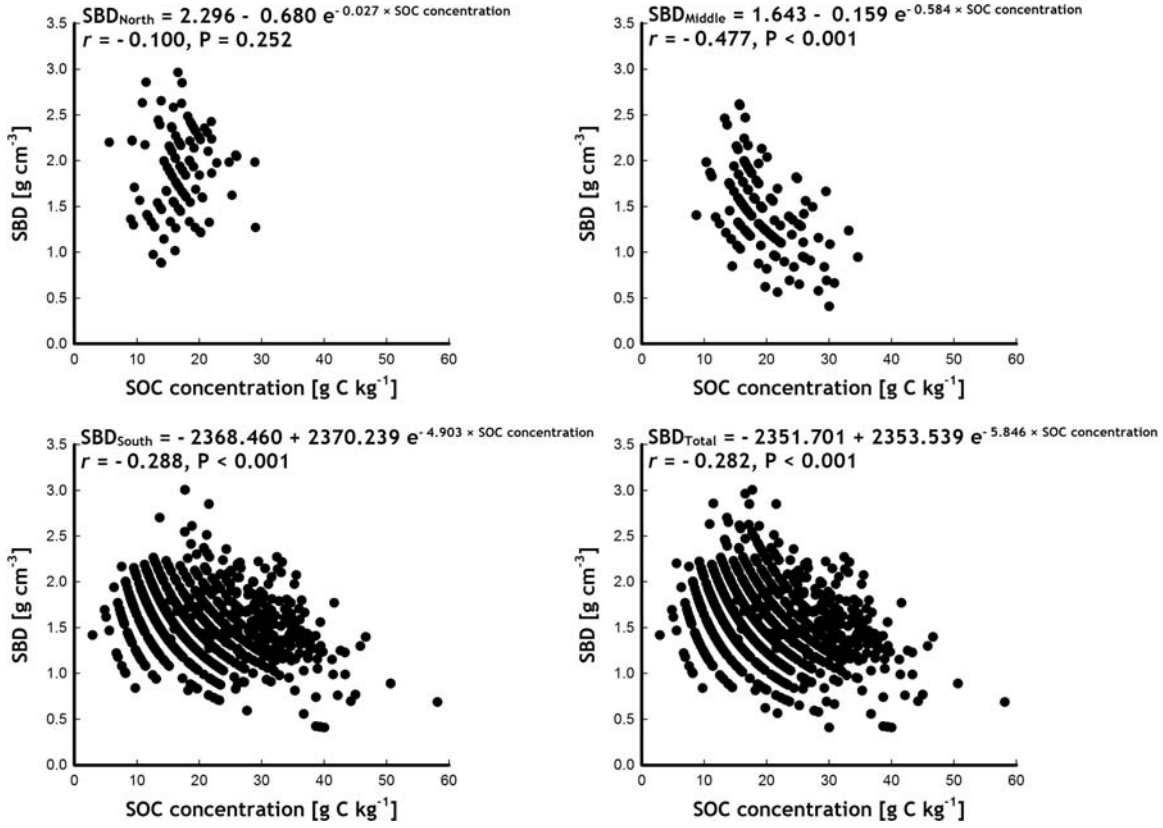

Figure 7 Non-linear correlation between sediment organic carbon [SOC] concentration [g C kg^{-1}] and sediment bulk density [SBD, g cm^{-3}] for sediment samples from three locations of *Avicennia marina* populations along the Red Sea coast of Saudi Arabia.

to shift more energy to osmotic regulation within the plant and reducing energy in plant growth (Alongi, 2014; Mizanur Rahman et al., 2015); this added stress ultimately leads to a decrease in leaf and stem production, making them less available to become incorporated into the sediments (Arshad et al., 2018). Vaiphasa et al. (2007) reported that shrimp pond effluents had dramatic effects on the survival of mangroves surrounding the ponds, where it has been reported that the disposal of nutrients (e.g., N and P) can accelerate the decomposition of mangrove SOM and thereby reduce SOC pools (Feller et al., 2003; Suárez-Abelenda et al., 2014). Moreover, Arshad et al. (2018) showed that sewage discharge lead to death of pneumatophores, which have been shown to affect mangrove productivity. The death of pneumatophores decreases the aeration area which apparently affects the respiration rate of the root system, nutrient uptake and plant growth, consequently leading to retarded growth of mangroves (Mandura, 1997). In the current study, seawater analysis reflected decreasing gradients of EC and TDS from the north to the south. The middle location was characterized by the highest concentrations of total P and total N, while the northern location had the lowest. These results are consistent with the studies of Saifullah (1997), Alongi (2011) and Triantafyllou et al. (2014).

The inverse relationship between density and the size of *A. marina* individuals in the middle location (highest density versus smallest size), as found by the present study, may be partially related to the effect of intraspecific competition (Shaltout and Ayyad, 1988). Plants with neighbours close by will grow less than plants with few or distant neighbours (Weiner, 1984). However, assessing the effect of intraspecific competition on the population dynamics of *A. marina* along the Saudi Arabian Red Sea coast, needs further field and experimental studies. In addition, the patchy distribution and stunting nature of mangroves in this location may also be due to dry land, paucity of rainfall, land use changes and high concentrations of P and N in the seawater due to the discharge of sewage and fertilizers (Almahasheer et al., 2017; Alongi, 2011; Kumar et al., 2010; Naidoo, 2009; Saifullah, 1997). On the other hand, the largest mangroves were recorded in the southern location, but they were associated with a relatively low population density; this may be partially due to a decrease in intraspecific competition that often leads to an increase in plant size. The present study showed that the density of *A. marina* was positively correlated with total N and total P. Thus, the relatively low concentrations of N and P in the seawater in the southern location may explain the relatively low density of mangroves trees at this location compared with the middle location (Sato et al., 2011).

SBD is a dynamic feature that differs with structural conditions within the sediment. SBD is the dry weight of specific sediment volume (Pravin et al., 2013); it is used as an indicator of sediment strength and/or mechanical resistance to plant growth and is used as a first step in evaluating SOC concentrations (Drewry et al., 2008). Our results showed that SBD gradually increased with depth in all the studied locations; this finding is consistent with those of Eid and Shaltout (2016) along the Egyptian Red Sea coast, and Eid et al. (2016)

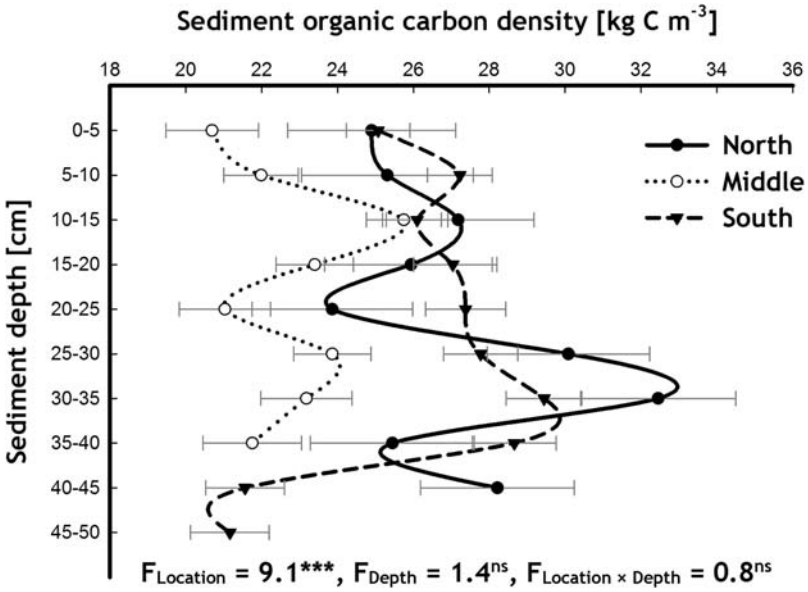

Figure 8 Distribution of sediment organic carbon density [kg C m^{-3}] in relation to sediment depth [cm] in three locations of *Avicennia marina* populations along the Red Sea coast of Saudi Arabia. Horizontal bars indicate the standard errors of the means. *F*-values represent the two-way ANOVAs. Location: North/Middle/South; Depth: 0–5, 5–10, 10–15, 15–20, 20–25, 25–30, 30–35, 35–40, 40–45, 45–50 cm. ***: $P < 0.001$, *ns*: not significant [i.e., $P > 0.05$].

and Arshad et al. (2018) along the southern Saudi Arabian Red Sea coast. This behaviour of SBD can be attributed to the accumulation of tailings and plant remains in the surface and sub-surface layers of the sediments (Sherry et al., 1998), which lead to changes in the organic matter content, porosity and compaction (Pravin et al., 2013).

SOC concentrations in mangrove forests originate from local mangrove production (litter falls and underground roots: autochthonous; Alongi, 1998), trapped seaweeds and seagrasses (Mandura et al., 1988), benthic algae (Yong et al., 2011), and the tidal flux from adjacent coastal environments (allochthonous; Allison et al., 2003), which is subsequently deposited within the mangroves (Bouillon et al., 2003; Chen et al., 2012). There were gradual decreases in SOC concentrations in all locations of the study area, from surface sediments where most carbon inputs occur to the deeper sediment layers. Eid and Shaltout (2016), Eid et al. (2016) and Arshad et al. (2018) reported a similar pattern for *A. marina* sediments in the Egyptian and Saudi Arabian Red Sea mangroves. In addition, Schile et al. (2017) reported a similar pattern for mature (*A. marina*) and planted (*A. germinans*) mangrove sediments along 600 km of coastline in the United Arab Emirates. The variation in SOC concentrations with depth may be due to the interaction of complex processes such as hydrologic/sediment regimes, decomposition, biological cycling, leaching, illuviation, soil erosion, weathering of minerals, and atmospheric deposition (Girmay and Singh, 2012; Sanderman et al., 2018).

The mean SOC concentration in our study (16.1 g C kg^{-1}) was lower than the global mean value (22.0 g C kg^{-1}; Kristensen et al., 2008), and it was lower than that of mangrove forests in many other countries (Table 4) such as Australia, Thailand, Indonesia, Palau, Mexico, Brazil, and Micronesia; however, it is higher than reported values in Egypt, China, Japan, India, and Vietnam. The global variations in mangrove SOC concentrations are driven by specific regional carbon dynamics (Twilley et al., 2018). Thus, the low SOC concentrations in the study area may be attributed to an absence of riverine sediments and organic matter along the coasts and in the seawater due to the lack of rivers (Almahasheer et al., 2017), a rocky ground and a low population density of mangroves in the north, stunted trees and pollution in the middle and the relatively high SBD in the north and south.

In the current study, we developed negative exponential functions for the studied locations, where SBD increased while SOC decreased with soil depth. Comparable results were reported by Yang et al. (2014) for mangrove coasts of the Leizhou Peninsula (southern China), by Eid et al. (2016) and Arshad et al. (2018) for mangrove sediments along the Red Sea in southern Saudi Arabia, by Schile et al. (2017) for sediments of mature and planted mangroves along the coastline in the United Arab Emirates, by Eid and Shaltout (2016) for mangrove sediments along the Egyptian Red Sea coast, and by Donato et al. (2011) for mangrove sediments in the tropics. It is also consistent with the study of Pravin et al. (2013), who reported that the increase in organic matter leads to decreased bulk density of soil.

The current study showed that SOC density significantly declined with depth, which is consistent with many previous studies such as that of Arshad et al. (2018), Almahasheer et al. (2017) and Eid et al. (2016). Additionally, the mean SOC density for mangroves sediments of the Saudi Arabian Red Sea coast, as estimated in the present study (25.6 kg C m^{-3}), was lower than those of mangrove forests in many regions, such as estuarine mangroves sediments (38.0 kg C m^{-3}), oceanic mangroves sediments (61.0 kg C m^{-3}), Rookery Bay in Florida (510.0 kg C m^{-3}) and Abu Dhabi, UAE (1200.0 kg C m^{-3}) (Almahasheer et al., 2017). In addition, the mean SOC density in the present study was higher than that of Kosrae Island mangroves (23.0 kg C m^{-3}; Almahasheer et al., 2017) and some Egyptian mangroves (21.4 kg C m^{-3}; Eid and Shaltout, 2016). The relatively low SOC density along the Saudi Arabian

Table 4 Mean of sediment organic carbon [SOC] concentration [g C kg^{-1}] and SOC pool [kg C m^{-2}] in the *Avicennia marina* locations along the Red Sea coast of Saudi Arabia compared with those reported in different mangrove forests around the globe.

Location	SOC concentration	SOC pool	Depth [cm]	Reference
Red Sea coast, Saudi Arabia	16.1	9.2	50	Present study
Central Saudi Red Sea coast	6.0	4.3	100	Almahasheer et al. (2017)
Arabian Gulf, United Arab Emirates		10.2–15.6	100	Schile et al. (2017)
Red Sea coast, Egypt	15.7	8.6	40	Eid and Shaltout (2016)
Africa Sahel, Senegal		9.0	40	Woomer et al. (2004)
Arid Western Australia	37.0	14.4	100	Alongi et al. (2000), Alongi et al. (2003)
Ao Sawi, Thailand	39.2		100	Alongi et al. (2001)
Fujian province, Southeastern China	11.3		60	Xue et al. (2009)
Leizhou Peninsula, China	9.5	8.7	100	Yang et al. (2014)
Shenzhen Bay, China	1.1–61.4	6.6	100	Lunstrum and Chen (2014)
Okinawa Island, Japan	7.7–20.1	5.7	100	Khan et al. (2007)
Sundarbans, India	6.1	2.6	30	Ray et al. (2011)
Xuan Thuy National Park, Vietnam	7.8		2	Tue et al. (2012)
Segara Anakan Lagoon, Kongsi Island and Thousand Islands, Indonesia	42.4	39.1	100	Kusumaningtyas et al. (2019)
La Paz Bay, Mexico		10.0–23.9	45	Ochoa-Gómez et al. (2019)
Karastic coastal region, Mexico	168.9	48.4	100	Adame et al. (2013)
Tamandaré, Brazil	58.4		46	Sanders et al. (2010)
Sepetiba Bay, Brazil	36.5		15	Lacerda et al. (1995)
Ceará State, Brazil		8.2	40	Nóbrega et al. (2019)
Sao Paulo, Brazil	210.6		80	Ferreira et al. (2010)
Ruunuw mangrove forest, Micronesia	104.3	12.1	100	Kauffman et al. (2011)
Airai mangrove forest, Palau	182.6	56.7	100	Kauffman et al. (2011)

Red Sea coast may be due to certain habitat characteristics and geomorphological settings that are not favourable for organic carbon sequestration (Almahasheer et al., 2017).

The current results indicate that the SOC pool in the middle location (6.7 kg C m^{-2}) was lower than that in the northern (10.5 kg C m^{-2}) and southern (10.4 kg C m^{-2}) location, proving that anthropogenic factors resulting from the industrial and urban expansion in the middle location in recent years, played a significant role in the SOC pool value (Almahasheer et al., 2017; Arshad et al., 2018). Moreover, the mean SOC pool in southern locations (10.4 kg C m^{-2}) in the present study was found to be below that mean reported (29.2 kg C m^{-2}) by Eid et al. (2019) in three homogenous sites near Jazan. This is clearly related to different sampling depths as they sampled sediments to 100 cm depth, while in the current study, the sediments were sampled to a 50 cm depth from five heterogeneous sites (Amaq, Al-Birk, Al-Shuqaiq, Sabya and Jazan). The low SOC pool capacity of Red Sea mangroves, especially in the middle part of the coast, may also be attributed to severe environmental conditions, leading to limited mangrove growth with dwarfed trees and a low biomass (Almahasheer et al., 2016b,c).

In the present study, the sediment profile in the mangrove forests along the Saudi Arabian Red Sea coast (0–50 cm) had a mean SOC pool of 9.2 kg C m^{-2}, which was lower than that of Indonesian, Palauan, Mexican, Australian and Micronesian mangrove sediments (Table 4) at a depth of 100 cm. On the other hand, it was higher than Egyptian mangrove sediments at a depth of 40 cm depth. This hemispheric variation in SOC pools is due to local and regional geomorphic and geophysical drivers (Rovai et al., 2018; Twilley et al., 2018), vegetation type or density, forest age, anthropogenic impacts, tidal range, biotic influences, hydrology and climate (Nóbrega et al., 2019; Taillardat et al., 2018). Donato et al. (2011) added that the mangrove organic sediments can exceed a depth of 3 m in some places; thus, the SOC pool in the current study may underestimate the carbon sequestration capacity because we only sampled sediments to a depth of 50 cm.

The accumulation of organic carbon in soils is the result of a balance between the input of autochthonous material through primary production or the deposition of allochthonous material versus the output due to decomposition/mineralization, erosion, and leaching (see Nóbrega et al., 2019). In our study, the mean CSR of mangrove forests along the Saudi Arabian Red Sea coast is 5.6 g C m^{-2} yr^{-1}. This value is consistent with the value of Arshad et al. (2018), who reported an average CSR of 4.7 g C m^{-2} yr^{-1} in southern Saudi Red Sea mangrove sediments, and it is close to the value of Almahasheer et al. (2017), who reported an average CSR of 3.5 g C m^{-2} yr^{-1} in central Red Sea mangrove sediments. On the other hand, the average CSR of the current study (5.6 g C m^{-2} yr^{-1}) is 29.0-fold lower than the average value of 163.0 g C m^{-2} yr^{-1} of the mangroves at the global scale (Breithaupt et al., 2012). The relatively low CSR in Saudi Red Sea mangroves is most likely due to the oligotrophic nature of the Red Sea, the lack of rivers, the extremely arid conditions affecting mangrove growth (Almahasheer et al., 2017), the lower primary productivity in Red Sea mangrove forests (Arshad et al., 2018), and the heavy metal pollution that may negatively influence primary production (Arshad et al., 2018; Bouillon et al., 2008).

Despite the importance of mangrove forests and their effective role in carbon sequestration and mitigating climate change (Sanderman et al., 2018), mangrove forests are one of the most threatened and rapidly degraded natural environments in the world (Sanderman et al., 2018; Siikamäki et al., 2012). Although Almahasheer et al. (2016a) stated that the area of mangrove forests along the Red Sea coasts have increased by 12% over the past forty years due to the efforts of local authorities, mangrove trees in the Red Sea still face many threats such as the establishment of resorts, oil industry development, overcutting, overgrazing (Hussain and Khojat, 1993), oil and sewage pollution (Shaltout et al., 2018), and the conversion of mangrove forests into shrimp farms (Eid et al., 2019). Therefore, in 2017, a decree was issued by the Council of Ministers of Saudi Arabia to form the Standing Committee for the Protection of the Environment of Coastal Areas. One of the tasks of this committee is to protect mangrove environments. Based on the area of mangrove stands along the Saudi Arabian Red Sea coast (48.4 km^2) and CSR, the total CSP of mangrove forests distributed along the Saudi Arabian Red Sea coast is 0.27 Gg C yr^{-1}. The relatively low CSP of Saudi Arabian Red Sea mangroves may be due to harsh environmental conditions such as low rainfall and high temperatures. Moreover, the sediments are composed mainly of biogenic coarse carbonates making the contribution of Saudi Arabian Red Sea mangroves to the carbon sequestration process limited (Almahasheer et al., 2017). It is, therefore, necessary to protect Saudi Arabian Red Sea mangrove ecosystems to improve their carbon sequestration potential and to benefit the other ecosystem services that they offer.

5. Limitations and uncertainties

To explore the effect of nutrient availability and salinity gradients on mangrove forests, the present study was conducted at 3 locations (northern, middle and southern), 7 sites and in 21 stands of mangrove forests (*A. marina*) along ~1134 km of the arid climate of the Saudi Arabian Red Sea coast. Although EC, TDS, total P and total N were determined in 3 seawater samples, which were collected from each stand to represent the nutrient availability and salinity gradients, factors other than EC, TDS, total P and total N might have also contributed to the differences in sediment (SBD, SOC concentration, SOC density, SOC pool and CSR) parameters among the locations. These factors include the geomorphologic settings, tidal input, human interference, seasonal variations (which play a role in changing the carbon dynamics in arid mangroves; Ray and Weigt, 2018) and finally methodological assumptions that were made in the manuscript: the relation between organic matter and organic carbon (SOM vs. SOC) and a constant sedimentation rate in the investigated sites. Thus, future research should examine the effects of each of the abovementioned factors on carbon dynamics of mangroves in greater detail.

Acknowledgements

The authors extend their appreciation to the Deanship of Scientific Research at King Khalid University for funding this work through General Research Project under grant number G.R.P. 117—39. We thank Dr. M.A. Al-Faidi and Dr. N.A. Al-Harbi (Biology Department, College of Science, Tabuk University); and Dr. M.A. Taher (Biology Department, College of Science, King Khalid University), for their valuable help during the field work.

Appendix A. Supplementary data

Supplementary material related to this article can be found, in the online version, at doi:10.1016/j.oceano.2019.08.002.

References

Adame, M.F., Kauffman, J.B., Boone, J., Medina, I., Gamboa, J.N., Torres, O., Caamal, J.P., Reza, M., Herrera-Silveira, J.A., 2013. Carbon stocks of tropical coastal wetlands within the karstic landscape of the Mexican Caribbean. PLoS One 8 (2), e56569.

Allison, M.A., Khan, S.R., Goodbred Jr., S.L., Kuehl, S.A., 2003. Stratigraphic evolution of the late Holocene Ganges-Brahmaputra lower delta plain. Sediment Geol. 155 (3—4), 317—342.

Almahasheer, H., 2018. Spatial coverage of mangrove communities in the Arabian Gulf. Environ. Monit. Assess. 190 (2), art. no. 85, 10 pp., http://dx.doi.org/10.1007/s10661-018-6472-2.

Almahasheer, H., Aljowair, A., Duarte, C.M., Irigoien, X., 2016a. Decadal stability of Red Sea mangroves. Estuar. Coast. Shelf Sci. 169, 164—172, http://dx.doi.org/10.1016/j.ecss.2015.11.027.

Almahasheer, H., Duarte, C., Irigoien, X., 2016b. Nutrient limitation in central Red Sea mangroves. Front. Mar. Sci. 3 , art. no. 271, 14 pp., http://dx.doi.org/10.3389/fmars.2016.00271.

Almahasheer, H., Duarte, C., Irigoien, X., 2016c. Phenology and growth dynamics of *Avicennia marina* in the central Red Sea. Sci. Rep. 6 (1), art. no. 37785, 9 pp., http://dx.doi.org/10.1038/srep37785.

Almahasheer, H., Serrano, O., Duarte, C., Arias-Ortiz, A., Masque, P., Irigoien, X., 2017. Low carbon sink capacity of Red Sea mangroves. Sci. Rep. 7 (1), art. no. 9700, 10 pp., http://dx.doi.org/10.1038/s41598-017-10424-9.

Alongi, D., Tirendi, F., Clough, B., 2000. Below-ground decomposition of organic matter in forests of the mangroves *Rhizophora stylosa* and *Avicennia marina* along the arid coast of Western Australia. Aquat. Bot. 68 (2), 97—122, http://dx.doi.org/10.1016/S0304-3770(00)00110-8.

Alongi, D., Wattayakorn, G., Pfitzner, J., Tirendi, F., Zagorskis, I., Brunskill, G., Davidson, A., Clough, B., 2001. Organic carbon accumulation and metabolic pathways in sediments of mangrove forests in southern Thailand. Mar. Geol. 179 (1—2), 85—103, http://dx.doi.org/10.1016/S0025-3227(01)00195-5.

Alongi, D.M., Clough, B.F., Dixon, P., Tirendi, F., 2003. Nutrient partitioning and storage in arid-zone forests of the mangroves *Rhizophora stylosa and Avicennia marina*. Trees 17 (1), 51-60, http://dx.doi.org/10.1007/s00468-002-0206-2.

Alongi, D.M., 1998. Coastal Ecosystem Processes. CRC Press, Florida, 448 pp.

Alongi, D.M., 2011. Early growth responses of mangroves to different rates of nitrogen and phosphorus supply. J. Exp. Mar. Biol. Ecol. 397 (2), 85—93, http://dx.doi.org/10.1016/j.jembe.2010.11.021.

Alongi, D.M., 2012. Carbon sequestration in mangrove forests. Carbon Manage. 3 (3), 313—322, http://dx.doi.org/10.4155/cmt.12.20.

Alongi, D.M., 2014. Carbon cycling and storage in mangrove forests. Annu. Rev. Mar. Sci. 6 (1), 195—219, http://dx.doi.org/10.1146/annurev-marine-010213-135020.

Arshad, M., Alrumman, S., Eid, E.M., 2018. Evaluation of carbon sequestration in the sediment of polluted and non-polluted locations of mangroves. Fund. Appl. Limnol. 192 (1), 53—64, http://dx.doi.org/10.1127/fal/2018/1127.

Bouillon, S., Borges, A., Casteneda-Moya, E., Diele, K., Dittmar, T., 2008. Mangrove production and carbon sinks: a revision of global budget estimates. Global Biogeochem. Cy. 22 (2), art. no. GB2013, 12 pp., http://dx.doi.org/10.1029/2007GB003052.

Bouillon, S., Dahdouh-Guebas, F., Rao, A.V.V.S., Koedam, N., Dehairs, F., 2003. Sources of organic carbon in mangrove sediments: variability and possible ecological implications. Hydrobiologia 495 (1—3), 33—39, http://dx.doi.org/10.1023/A:1025411506526.

Breithaupt, J., Smoak, J., Smith, T., Sanders, C., Hoare, A., 2012. Organic carbon burial rates in mangrove sediments: strengthening the global budget. Global Biogeochem. Cy. 26 (3), art. no. GB3001, 11 pp., http://dx.doi.org/10.1029/2012GB004375.

Bunting, P., Rosenqvist, A., Lucas, R.M., Rebelo, L.-M., Hilarides, L., Thomas, N., Hardy, A., Itoh, T., Shimada, M., Finlayson, C.M., 2018. The global mangrove watch — a new 2010 global baseline of mangrove extent. Remote Sens. 10 (1), art. no. 1669, http://dx.doi.org/10.3390/rs10101669.

Chen, L., Zeng, X., Tam, N.F.Y., Lu, W., Luo, Z., Du, X., Wang, J., 2012. Comparing carbon sequestration and stand structure of monoculture and mixed mangrove plantations of *Sonneratia caseolaris* and *S. apetala* in Southern China. Forest Ecol. Manage. 284, 222—229, http://dx.doi.org/10.1016/j.foreco.2012.06.058.

Donato, D., Kauffman, J., Murdiyarso, D., Kurnianto, S., Stidham, M., Kanninen, M., 2011. Mangroves among the most carbon-rich forests in the tropics. Nat. Geosci. 4 (5), 293—297, http://dx.doi.org/10.1038/ngeo1123.

Drewry, J.J., Cameron, K.C., Buchan, G.D., 2008. Pasture yield and soil physical property responses to soil compaction from treading and grazing — a review. Aust. J. Soil Res. 46 (3), 237—256, http://dx.doi.org/10.1071/SR07125.

Edwards, A.J., Head, S.M., 1987. Key Environment: Red Sea. Pergamon Press, Headington Hill Hall, Oxford, 451 pp., http://dx.doi.org/10.1016/C2009-0-07683-1.

Edwards, F.J., 1987. Climate and oceanography. In: Edwards, A.J., Head, S.M. (Eds.), Key Environment: Red Sea. Pergamon Press, New York, 45—69.

Eid, E.M., Arshad, M., Shaltout, K.H., El-Sheikh, M.A., Alfarhan, A.H., Picó, Y., Barcelo, D., 2019. Effect of the conversion of mangroves into shrimp farms on carbon stock in the sediment along the southern Red Sea coast, Saudi Arabia. Environ. Res. 176, art. no. 108536, 7 pp., http://dx.doi.org/10.1016/j.envres.2019.108536.

Eid, E.M., El-Bebany, A.F., Alrumman, S.A., 2016. Distribution of soil organic carbon in the mangrove forests along the southern Saudi Arabian Red Sea coast. Rend. Fis. Acc. Lincei. 27 (4), 629—637, http://dx.doi.org/10.1007/s12210-016-0542-6.

Eid, E.M., Shaltout, K.H., 2016. Distribution of soil organic carbon in the mangrove *Avicennia marina* (Forssk.) Vierh. along the Egyptian Red Sea coast. Reg. Stud. Mar. Sci. 3, 76—82, http://dx.doi.org/10.1016/j.rsma.2015.05.006.

El-Juhany, L.I., 2009. Present status and degradation trends of mangrove forests on the southern Red Sea coast of Saudi Arabia. Am. Euras. J. Agric. Environ. Sci. 6 (3), 328—340.

Feller, I.C., McKee, K.L., Whigham, D.F., O'Neill, J.P., 2003. Nitrogen vs. phosphorus limitation across an ecotonal gradient in a mangrove forest. Biogeochemistry 62 (2), 145—175, http://dx.doi.org/10.1023/A:1021166010892.

Ferreira, T.O., Otero, X.L., de Souza Junior, V.S., Vidal-Torrado, P., Macías, F., Firme, L.P., 2010. Spatial patterns of soil attributes and components in a mangrove system in Southeast Brazil (São Paulo). J. Soils Sediments 10 (6), 995—1006, http://dx.doi.org/10.1007/s11368-010-0224-4.

Girmay, G., Singh, B.R., 2012. Changes in soil organic carbon stocks and soil quality: land-use system effects in northern Ethiopia. Acta Agric. Scand., Sect. B - Soil Plant Sci. 62 (6), 519—530, http://dx.doi.org/10.1080/09064710.2012.663786.

Han, F., Hu, W., Zheng, J., Du, F., Zhang, X., 2010. Estimating soil organic carbon storage and distribution in a catchment of Loess Plateau, China. Geoderma 154 (3—4), 261—266, http://dx.doi.org/10.1016/j.geoderma.2009.10.011.

Hussain, M., Khojat, T., 1993. Intertidal and subtidal blue-green algal mats of open and mangrove areas in the Farasan Archipelago (Saudi Arabia), Red Sea. Bot. Mar. 36 (5), 377—388, http://dx.doi.org/10.1515/botm.1993.36.5.377.

Jones, J.B., 2001. Laboratory Guide for Conducting Soil Tests and Plant Analysis. CRC Press, Florida, 384 pp.

Kauffman, J.B., Heider, C., Cole, T.G., Dwire, K.A., Donato, D.C., 2011. Ecosystem carbon stocks of Micronesian mangrove forests. Wetlands 31 (2), 343—352, http://dx.doi.org/10.1007/s13157-011-0148-9.

Khan, M., Suwa, R., Hagihara, A., 2007. Carbon and nitrogen pools in a mangrove stand of *Kandelia obovata* (S., L.) Yong: vertical distribution in the soil-vegetation system. Wetlands Ecol. Manage. 15 (2), 141—153, http://dx.doi.org/10.1007/s11273-006-9020-8.

Kristensen, E., Bouillon, S., Dittmar, T., Marchand, C., 2008. Organic carbon dynamics in mangrove ecosystems: a review. Aquat. Bot. 89 (2), 201—219, http://dx.doi.org/10.1016/j.aquabot.2007.12.005.

Kumar, A., Asif Khan, M., Muqtadir, A., 2010. Distribution of mangroves along the Red Sea Coast of the Arabian Peninsula: Part-I: the Northern Coast of Western Saudi Arabia. Earth Sci. India 3 (3), 28—42.

Kusumaningtyas, M.A., Hutahaean, A.A., Fischer, H.W., Pérez-Mayo, M., Ransby, D., Jennerjahn, T.C., 2019. Variability in the organic carbon stocks, sources, and accumulation rates of Indonesian mangrove ecosystems. Estuar. Coast. Shelf Sci. 218, 310—323, http://dx.doi.org/10.1016/j.ecss.2018.12.007.

Lacerda, L., Ittekkot, V., Patchineelam, S., 1995. Biogeochemistry of mangrove soil organic matter: a comparison between *Rhizophora* and *Avicennia* soils in south-eastern Brazil. Estuar. Coast. Shelf Sci. 40 (6), 713—720, http://dx.doi.org/10.1006/ecss.1995.0048.

Lovelock, C., Feller, I., McKee, K., Engelbrecht, B., Ball, M., 2004. The effect of nutrient enrichment on growth, photosynthesis and hydraulic conductance of dwarf mangroves in Panama. Funct. Ecol. 18 (1), 25—33, http://dx.doi.org/10.1046/j.0269-8463.2004.00805.x.

Lunstrum, A., Chen, L., 2014. Soil carbon stocks and accumulation in young mangrove forests. Soil Biol. Biochem. 75, 223—232, http://dx.doi.org/10.1016/j.soilbio.2014.04.008.

Mandura, A.S., 1997. A mangrove stand under sewage pollution stress: Red Sea. Mangroves Salt Marshes 1 (4), 255—262, http://dx.doi.org/10.1023/A:1009927605517.

Mandura, A.S., Khafaji, A.K., Saifullah, S.M., 1988. Ecology of a mangrove stand of a central Red Sea coast area: Ras Hatiba (Saudi Arabia). Proc. Saudi Biol. Soc. 11, 85—112.

Mandura, A.S., Khafaji, A.K., Saifullah, S.M., 1987. Mangrove ecosystem of southern Red Sea coast of Saudi Arabia. Proc. Saudi Biol. Soc. 10, 165—193.

Meersmans, J., De Ridder, F., Canters, F., De Baets, S., Van Molle, M., 2008. A multiple regression approach to assess the spatial distribution of soil organic carbon (SOC) at the regional scale (Flanders Belgium). Geoderma 143 (1—2), 1—13, http://dx.doi.org/10.1016/j.geoderma.2007.08.025.

Mizanur Rahman, M., Nabiul Islam Khan, M., Fazlul Hoque, A.K., Ahmed, I., 2015. Carbon stock in the Sundarbans mangrove forest: spatial variations in vegetation types and salinity zones. Wetlands Ecol. Manag. 23 (2), 269—283, http://dx.doi.org/10.1007/s11273-014-9379-x.

Morley, N.J.F., 1975. The coastal waters of the Red Sea. Bull. Mar. Res. Cen. 5, 8—19.

Naidoo, G., 2009. Differential effects of nitrogen and phosphorus enrichment on growth of dwarf *Avicennia marina* mangroves. Aquat. Bot. 90 (2), 184—190, http://dx.doi.org/10.1016/j.aquabot.2008.10.001.

Nóbrega, G.N., Ferreira, T.O., Artur, A.G., Mendonça, E.S., Leão, R. A., Teixeira, A.S., Otero, X.L., 2015. Evaluation of methods for quantifying organic carbon in mangrove soils from semi-arid region. J. Soil. Sediment. 15 (2), 282—291, http://dx.doi.org/10.1007/s11368-014-1019-9.

Nóbrega, G.N., Ferreira, T.O., Neto, M.S., Mendonça, E.S., Romero, R.E., Otero, X.L., 2019. The importance of blue carbon soil stocks in tropical semiarid mangroves: a case study in Northeastern Brazil. Environ. Earth Sci. 78 (12), art. no. 369, 10 pp., http://dx.doi.org/10.1007/s12665-019-8368-z.

Novozamsky, I., van Eck, R., van Schouwenburg, J., Walinga, I., 1974. Total nitrogen determination in plant material by means of the indophenol blue method. Neth. J. Agric. Sci. 22, 3—13.

Ochoa-Gómez, J.G., Lluch-Cota, S.E., Rivera-Monroy, V.H., Lluch-Cota, D.B., Troyo-Diéguez, E., Oechel, W., Serviere-Zaragoza, E., 2019. Mangrove wetland productivity and carbon stocks in an arid zone of the Gulf of California (La Paz Bay, Mexico). Forest Ecol. Manage. 442, 135—147, http://dx.doi.org/10.1016/j.foreco.2019.03.059.

Page, M.L., 2019. Carbon dioxide levels will soar past the 410 ppm milestone in 2019. NewScientist 3214.

Pravin, R., Dodha, V., Vidya, D., Manab, C., Saroj, M., 2013. Soil bulk density as related to soil texture, organic matter content and available total nutrients of Coimbatore soil. IJSRP 3 (2), 1—8.

Pribyl, D.W., 2010. A critical review of the conventional SOC to SOM conversion factor. Geoderma 156 (3—4), 75—83, http://dx.doi.org/10.1016/j.geoderma.2010.02.003.

Price, A., Jobbins, G., Dawson Shepherd, A., Ormond, R., 1998. An integrated environmental assessment of the Red Sea coast of Saudi Arabia. Environ. Conserv. 25 (1), 65—76, http://dx.doi.org/10.1017/S0376892998000101.

Price, A.R., Medley, P.A., McDowall, R.J., Dawson-Shepherd, A.R., Hogarth, P.J., Ormond, R.F., 1987. Aspects of mangal ecology along the Red Sea coast of Saudi Arabia. J. Nat. Hist. 21 (2), 449—464, http://dx.doi.org/10.1080/00222938700771121.

Ray, R., Ganguly, D., Chowdhury, C., Dey, M., Das, S., Dutta, M., Mandal, S., Majumder, N., De, T., Mukhopadhyay, S., Jana, T., 2011. Carbon sequestration and annual increase of carbon stock in a mangrove forest. Atmos. Environ. 45 (28), 5016—5024, http://dx.doi.org/10.1016/j.atmosenv.2011.04.074.

Ray, R., Weigt, M., 2018. Seasonal and habitat-wise variations of creek water particulate and dissolved organic carbon in arid mangrove (the Persian Gulf). Cont. Shelf Res. 165, 60—70, http://dx.doi.org/10.1016/j.csr.2018.06.009.

Rovai, A., et al., 2018. Global controls on carbon storage in mangrove soils. Nat. Clim. Change 8 (6), 534—538, http://dx.doi.org/10.1038/s41558-018-0162-5.

Rumpel, C., Amiraslani, F., Koutika, L.-S., Smith, P., Whitehead, D., Wollenberg, E., 2018. Put more carbon in soils to meet Paris climate pledges. Nature 564 (7734), 32—34, http://dx.doi.org/10.1038/d41586-018-07587-4.

Saifullah, S.M., 1994. Mangrove ecosystem of Saudi Arabian Red Sea coast — an overview. J. KAU: Mar. Sci. 7, 263—270.

Saifullah, S.M., 1997. Mangrove ecosystem of Red Sea coast (Saudi Arabian). Pak. J. Mar. Sci. 6 (1—2), 115—124.

Sanderman, J., Hengl, T., Fiske, G., Solvik, K., Adame, M., Benson, L., Bukoski, J., Carnell, P., Cifuentes-Jara, M., Donato, D., Duncan, C., Eid, E., zu Ermgassen, P., Ewers Lewis, C., Macreadie, P., Glass, L., Gress, S., Jardine, S., Jones, T., Nsombo, E., Rahman, M., Sanders, C., Spalding, M., Landis, E., 2018. A global map of mangrove forest soil carbon at 30 m spatial resolution. Environ. Res. Lett. 13 (5), art. no. 055002, 12 pp., http://dx.doi.org/10.1088/1748-9326/aabe1c.

Sanders, C.J., Smoak, J.M., Naidu, A.S., Sanders, L.M., Patchineelam, S.R., 2010. Organic carbon burial in a mangrove forest, margin and intertidal mud flat. Estuar. Coast. Shelf Sci. 90 (3), 168—172, http://dx.doi.org/10.1016/j.ecss.2010.08.013.

Sato, G., Negassi, S., Tahiri, A., 2011. The only elements required by plants that are deficient in sea water are nitrogen, phosphorous and iron. Cytotechnology 63 (2), 201—204, http://dx.doi.org/10.1007/s10616-011-9342-0.

Schile, L.M., Kauffman, J.B., Crooks, S., Fourqurean, J.W., Glavan, J., Megonigal, J.P., 2017. Limits on carbon sequestration in arid blue carbon ecosystems. Ecol. Appl. 27 (3), 859—874, http://dx.doi.org/10.1002/eap.1489.

Shaltout, K.H., 2016. Economic and Environmental Values of Mangroves in Arabic Region. In: Proc. The First Saudi Conference on Environment: Sustainable Management of Natural Resources, King Khalid University & Center of Prince Sultan Ben Abd El-Aziz for Environmental and Touristic Research and Studies. Abha, Saudi Arabia, 7—9 March 2016.

Shaltout, K.H., Ayyad, M., 1988. Structure and standing crop of Egyptian *Thymelaea hirsuta* populations. Vegetatio 74 (2—3), 137—142, http://dx.doi.org/10.1007/BF00044738.

Shaltout, K.H., El-Bana, M.I., Eid, E.M., 2018. Ecology of the Mangrove Forests along the Egyptian Red Sea Coast. LAP Lambert Acad. Publ., Saarbrücken, 168 pp.

Sherry, S., Ramon, A., Eric, M., Richard, E., Barry, W., Peter, D., Susan, T., 1998. Precambrian shield wetlands: hydrologic control of the sources and export of dissolved organic matter. Clim. Change 40 (2), 167—188, http://dx.doi.org/10.1023/A:1005496331593.

Siikamäki, J., Sanchirico, J., Jardine, S., 2012. Global economic potential for reducing carbon dioxide emissions from mangrove loss. PANAS 109 (36), 14369—14374, http://dx.doi.org/10.1073/pnas.1200519109.

Siraj, A., 1984. Climate of Saudi Arabia. Fauna of Saudi Arabia 6, 32—52.

SPSS, 2006. SPSS Base 15.0 User's Guide. SPSS Inc., Chicago.

Strickland, J.D., Parsons, T.R., 1972. Determination of reactive phosphorus. In: A Practical Handbook of Seawater Analysis. Bull. Fisheries Res. Board Canada, no. 167, 49—56.

Suárez-Abelenda, M., Ferreira, T.O., Camps-Arbestain, M., Rivera-Monroy, V.H., Macías, F., Nóbrega, G.N., Otero, X.L., 2014. The effect of nutrient-rich effluents from shrimp farming on mangrove soil carbon storage and geochemistry under semi-arid climate conditions in northern Brazil. Geoderma 213, 551—559, http://dx.doi.org/10.1016/j.geoderma.2013.08.007.

Taillardat, P., Friess, D.A., Lupascu, M., 2018. Mangrove blue carbon strategies for climate change mitigation are most effective at the national scale. Biol. Lett. 14 (10), art. no. 20180251, 6 pp., http://dx.doi.org/10.1098/rsbl.2018.0251.

Tan, K.H., 2005. Soil Sampling, Preparation, and Analysis. Taylor & Francis Group, CRC Press, Florida, 672 pp., http://dx.doi.org/10.1201/9781482274769.

Ter Braak, C.J.F., Šmilauer, P., 2012. Canoco Reference Manual and User's Guide: Software for Ordination (Version 5.0). Microcomputer Power, Ithaca.

Triantafyllou, G., Yao, F., Petihakis, G., Tsiaras, K., Raitsos, D., Hoteit, I., 2014. Exploring the Red Sea seasonal ecosystem functioning using a three-dimensional biophysical model. J. Geophys. Res. Oceans 119 (3), 1791—1811, http://dx.doi.org/10.1002/2013JC009641.

Tue, N., Ngoc, N., Quy, T., Hamaoka, H., Nhuan, M., Omori, K., 2012. A cross-system analysis of sedimentary organic carbon in the mangrove ecosystems of Xuan Thuy National Park Vietnam. J. Sea Res. 67 (1), 69—76, http://dx.doi.org/10.1016/j.seares.2011.10.006.

Twilley, R.R., Rovai, A.S., Riul, P., 2018. Coastal morphology explains global blue carbon distributions. Front. Ecol. Environ. 16 (9), 1—6, http://dx.doi.org/10.1002/fee.1937.

Vaiphasa, C., de Boer, W.F., Skidmore, A.K., Panitchart, S., Vaiphasa, T., Bamrongrugsa, N., Santitamnont, P., 2007. Impact of solid shrimp pond waste materials on mangrove growth and mortality: a case study from Pak Phanang, Thailand. Hydrobiologia 591 (1), 47—57, http://dx.doi.org/10.1007/s10750-007-0783-6.

Weiner, J., 1984. Neighbourhood interference amongst *Pinus rigida* individuals. J. Ecol. 72 (1), 183—195, http://dx.doi.org/10.2307/2260012.

Wilke, B.M., 2005. Determination of chemical and physical soil properties. In: Margesin, R., Schinner, F. (Eds.), Manual for Soil Analysis-Monitoring and Assessing Soil Bioremediation. Springer, Heidelberg, 47—95.

Woomer, P.L., Tieszen, L.L., Tappan, G., Touré, A., Sall, M., 2004. Land use change and terrestrial carbon stocks in Senegal. J. Arid Environ. 59 (3), 625—642, http://dx.doi.org/10.1016/j.jaridenv.2004.03.025.

Xiaonan, D., Xiaoke, W., Lu, F., Zhiyun, O., 2008. Primary evaluation of carbon sequestration potential of wetlands in China. Acta. Ecol. Sinica 28 (2), 463—469, http://dx.doi.org/10.1016/S1872-2032(08)60025-6.

Xue, B., Yan, C., Lu, H., Bai, Y., 2009. Mangrove-derived organic carbon in sediment from Zhangjiang Estuary (China) mangrove wetland. J. Coast. Res. 25 (4), 949—956, http://dx.doi.org/10.2112/08-1047.1.

Yang, J., Gao, J., Liu, B., Zhang, W., 2014. Sediment deposits and organic carbon sequestration along mangrove coasts of the Leizhou Peninsula, southern China. Estuar. Coast. Shelf Sci. 136, 3—10, http://dx.doi.org/10.1016/j.ecss.2013.11.020.

Yong, Y., Baipeng, P., Guangcheng, C., Yan, C., 2011. Processes of organic carbon in mangrove ecosystems. Acta Ecol. Sinica 31 (3), 169—173, http://dx.doi.org/10.1016/j.chnaes.2011.03.008.